Composites Science and Technology 70 (2010) 291–297

Contents lists available at ScienceDirect

Composites Science and Technology

journal homepage: www.elsevier.com/locate/compscitech

A combined experimental–numerical approach for generating statistically equivalent fibre distributions for high strength laminated composite materials

T.J. Vaughan, C.T. McCarthy *

Composites Research Centre, Materials and Surface Science Institute (MSSI) and the Department of Mechanical and Aeronautical Engineering, University of Limerick, Limerick, Ireland

ARTICLE INFO

Article history:
Received 21 May 2009
Received in revised form 27 October 2009
Accepted 29 October 2009
Available online 4 November 2009

Keywords:
A. Polymer matrix composites
C. Statistics
C. Finite element analysis
D. Optical microscopy
Representative volume element

ABSTRACT

A technique is presented where actual experimental distributions, measured from a high strength carbon fibre composite, are considered in the development of a novel method to generate statistically equivalent fibre distributions for high volume fraction composites. The approach uses an adjusted measure of nearest neighbour distribution functions to define inter-fibre distances. The statistical distributions, characterising the resulting fibre arrangements, were found to be equivalent to those in the actual microstructure. Finite element models were generated and used to determine the effective elastic properties of the composite and excellent agreement was obtained. The algorithm developed is simple, robust, highly efficient and capable of reproducing actual fibre distributions for high strength laminated composite materials. It does not require further heuristic steps, such as those seen in fibre stirring/shaking algorithms, in order to achieve high volume fraction microstructures and provides a useful alternative to both microstructure reproduction and random numerical models.

1. Introduction

The increasing use of composite materials in the aerospace industry has heightened the need for more accurate computational methods to predict material behaviour. Composites fail due to various damage mechanisms occurring at the microscopic scale, including fibre fracture, fibre/matrix debonding and/or matrix micro-cracking. Multi-scale modelling is emerging as an effective technique to address these issues [1] whereby a micromechanical model in the form of a representative volume element (RVE) is coupled to a macro-mechanical model in order to predict behaviour. Micromechanical analysis of composite materials has conventionally been based on the assumption that the spatial arrangement of fibres in a composite microstructure is periodic. This approach leads to computationally efficient models, where effective properties can be accurately predicted. However, when applied to failure/damage related predictions, these simple models generally do not perform well [2] since damage is generally not periodic.

The spatial arrangement of fibres in a composite microstructure is in fact non-uniform and this can have a significant effect on the failure/damage properties under certain loading conditions. Trias et al. [3] compared the stress and strain distributions resulting from a transverse tensile load applied to both a random model and a periodic model of a carbon fibre composite. It was concluded that the use of periodic models could lead to an underestimation of matrix cracking and damage initiation and so the use of random models are needed when modelling failure and damage. Hojo et al. [4] investigated the effect of local fibre distributions on the microscopic interfacial normal stress states for unidirectional carbon fibre epoxy laminates loaded in transverse tension. It was found that for an irregular fibre array the absolute value of the interfacial normal stresses rapidly increased when the distance between fibres was less than 0.5 μm. It was also concluded that a periodic hexagonal model under the same loading conditions could not represent the microscopic stress state. Pyrz [5] found that in a polymer matrix composite, the overall failure stress is significantly influenced by the type of spatial pattern present. It is also shown that the nearest neighbour distances between fibres has a considerable effect on stress in the microstructure, with peak stresses occurring in regions where fibres lie in close proximity to one another.

The general approach taken to capture the non-uniform spatial arrangement of fibres within a composite microstructure is to develop a statistically equivalent RVE (SERVE). A SERVE is the smallest region of a generated microstructure which exhibits the same effective stress–strain behaviour as the overall composite. The distribution functions, reflecting the local morphology, should be equivalent to the actual microstructure and should be independent of location [2].

To generate a SERVE, the hard-core model (also known as the random sequential adsorption model) has been widely used [6,7]. This model represents the fibres as a set of non-overlapping disks, whose centres have been randomly distributed inside a square

* Corresponding author. Tel.: +353 61234334; fax: +353 61201944.
E-mail address: conor.mccarthy@ul.ie (C.T. McCarthy).

0266-3538/$ - see front matter © 2009 Elsevier Ltd. All rights reserved.
doi:10.1016/j.compscitech.2009.10.020

region. Yang et al. [7] used the hard-core model effectively to generate the non-uniform spatial arrangement of fibres in a ceramic matrix composite. Statistical functions were used to verify that the resulting distributions were equivalent to the real composite microstructure (which was experimentally characterised using digital image analysis). However, one of the constraints of the hard-core model is that it is subject to a jamming limit, which means it does not permit volume fractions greater than ~54% being generated [6]. Therefore, it cannot be used to represent the microstructure of high strength composite materials which generally have volume fractions in the region of 60%. To overcome this, Melro et al. [8] used an initial configuration generated by the hard-core model and then subjected the fibres to small arbitrary displacements, which created matrix rich regions. The presence of these areas allowed further fibres to be placed in the domain, resulting in fibre volume fractions of 65%. The resulting fibre arrangement was found to be described by a random distribution. Wongsto and Li [9] used an initial periodic hexagonal fibre array of the desired volume fraction and created a non-uniform fibre distribution by shifting the fibres through a random displacement. Trias [10] suggests an approach based on the random close packing of spheres. However, this method was found to be impractical due to the computational time needed to generate high volume fractions.

The above numerical approaches assume that the microstructure of a composite exhibits a random distribution of fibres. However, Pyrz [11] showed that for three different curing conditions applied to a glass/epoxy composite, the resulting spatial patterns in each microstructure differed considerably. It was concluded that the previous assumptions regarding complete randomness or perfect regularity in the microstructure may be in error and the patterns produced are highly dependant on the manufacturing process and conditions. It was also shown for the materials analysed that their probability density functions of nearest neighbour distances do not follow the same form as those of a complete spatial random (CSR) pattern. Trias [10] analysed the microstructures from four carbon fibre composites and found that the fibre distribution for three of these materials departed from a CSR pattern, each showing distinctive statistical distributions. It was concluded that because of the possible variance of statistical distributions from one composite material to another, a microstructural reproduction approach is more appropriate for micromechanical modelling than the use specific algorithms which are only capable of reproducing fibre distributions conforming to a CSR pattern.

This paper proposes a combined experimental–numerical approach for generating statistically equivalent representations of a high strength composite laminate. Because of the nature of high volume fraction composites, fibres are forced to arrange themselves in close proximity to one another, commonly at distances less than 0.5 μm. As shown in [4], this can result in a significant increase in the interfacial normal stresses being developed which is a key factor in transverse failure. Thus, the approach taken here uses experimentally measured nearest neighbour distribution functions to define the distances between fibres. This allows the generated distributions to replicate exactly the short range interactions of fibres. The material under study is HTA/6376, a high strength carbon fibre reinforced plastic (CFRP) used extensively in the aerospace industry. The microstructure has been analysed using digital image analysis, from which statistical data characterising the fibre arrangement has been found. The newly developed algorithm uses the diameter distribution to assign fibre diameters. The adjusted measure of both the 1st and 2nd nearest neighbour distribution functions are used to define the inter-fibre distances. The resulting high volume fraction fibre arrangements are statistically characterised and compared to the experimental samples. Finite element (FE) models are then used to determine the effective properties of the generated microstructures. It is shown that these models exhibit the same mechanical behaviour as the CFRP material.

2. Microstructure characterisation

Digital image analysis was carried out on a transverse cross-section of a 2 mm thick 16-ply unidirectional composite laminate using Buehler Omnimet imaging software. In order to characterise the microstructure of the composite material, 40 images, like that shown in Fig. 1a, were captured. Each measured 320 μm × 240 μm and contained approximately 1300 fibres. The software can automatically detect a colour 'threshold' level within each image and this allowed it to identify the fibres, as shown in Fig. 1b. From the image, the software extracted information such as fibre diameter and *x*,*y* coordinate of each fibre centre (note: only fibres which lay entirely in the view field were considered).

2.1. Statistical characterisation of CFRP microstructure

The data extracted from the digital image analysis was used to generate statistical functions that characterise the CFRP microstructure. Fig. 2a shows the distribution of fibre diameters, which conformed to a lognormal distribution, as shown. The mean fibre diameter is 6.6 μm and the fibre volume fraction (V_f) was computed as 59.2%. Many statistical descriptors exist which characterise the spatial point patterns [12] and these can be applied to the microstructural arrangement in composite materials by considering the positions of all fibre centres as a spatial point pattern. Three statistical descriptors are considered here which analyse both the

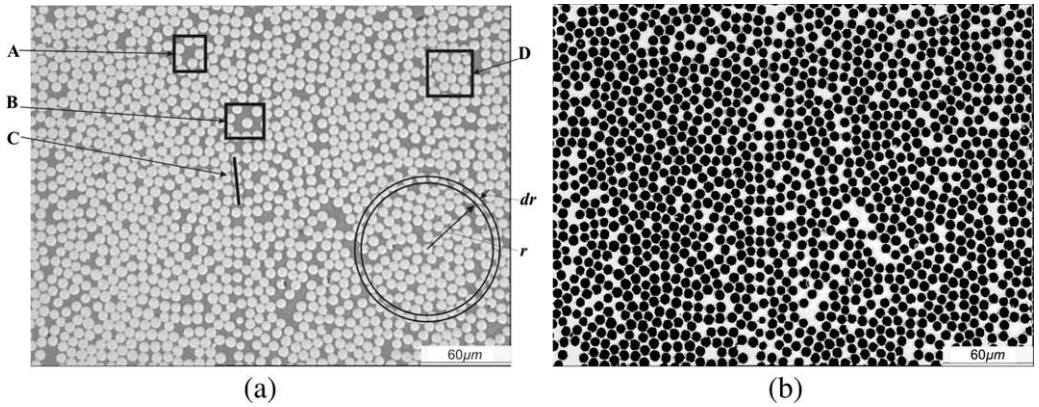

Fig. 1. Sample image chosen for analysis (320 μm × 240 μm): (a) actual micrograph, (b) computed microstructure based on a colour threshold algorithm.

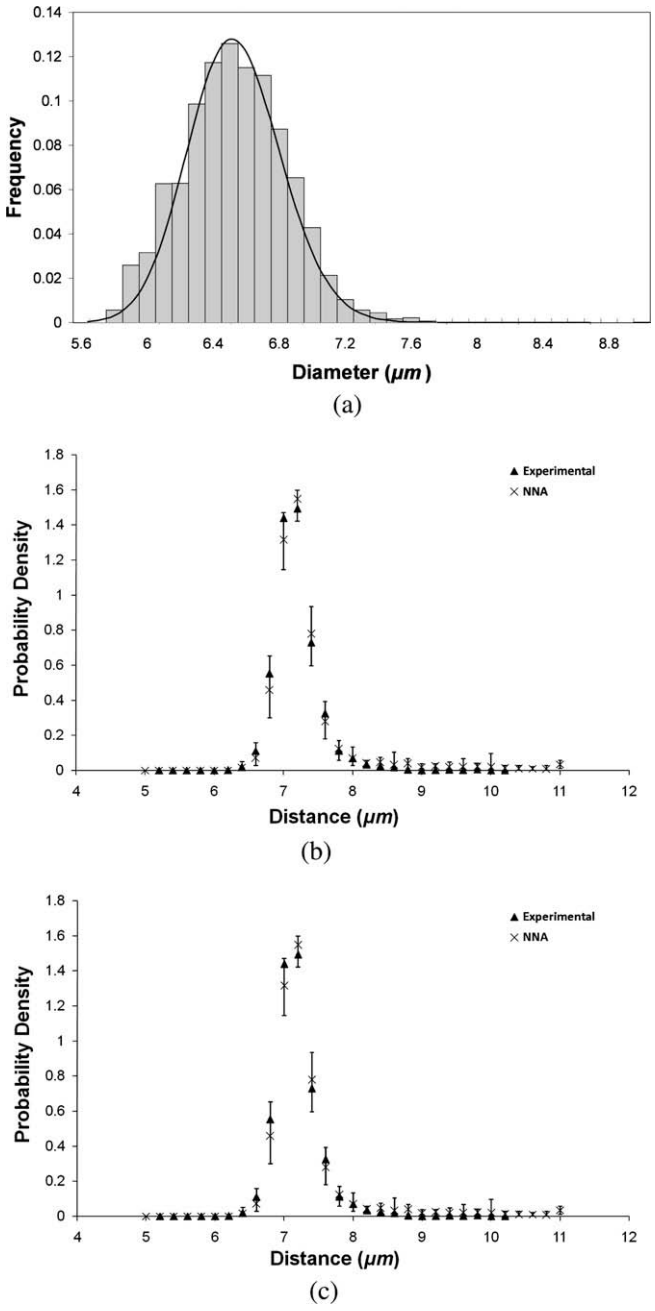

Fig. 2. (a) Size distribution of fibres. (b) 1st Nearest neighbour distribution function. (c) 2nd Nearest neighbour distribution function.

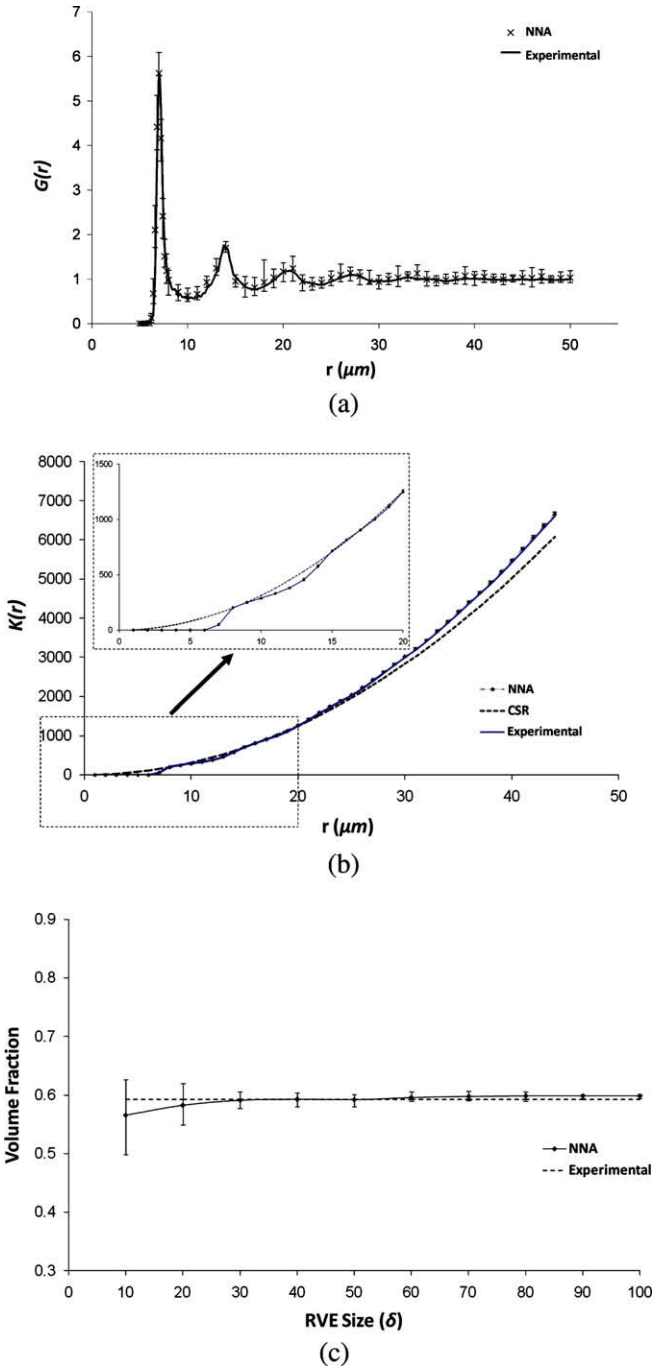

Fig. 3. (a) Radial distribution function. (b) Second-order intensity function. (c) Volume fraction size study.

short and long range interaction of inclusions and these are discussed below.

2.1.1. Nearest neighbour distribution

Nearest neighbour distribution functions detail the short range interaction between fibres by analysing the distance between each fibre and their *n*th closest neighbour [12]. Shown respectively in Fig. 2b and c is the 1st and 2nd nearest neighbour distributions of fibres. These distributions exhibit narrow ranges and high peaks occur at distances of 7 μm and 7.2 μm, respectively. From Fig. 2a, the mean of the diameter distribution was found to be 6.6 μm which implies that, for neighbouring fibres, the average inter-fibre spacing is in the region of 0.4 μm–0.6 μm. This minimal spacing between fibres has been shown by Hojo et al. [4] to have a significant effect on the stresses developed at the fibre/matrix interface under certain loading conditions, which will affect the overall failure properties of the composite. This further highlights the importance of reproducing these characteristics in a micromechanical model.

2.1.2. Radial distribution function

The radial distribution function, describes how the average fibre density varies as a function of distance from a given fibre centre. It is found by determining the number of fibres lying within an annular region, as shown in Fig. 1a, of inner radius, r, and outer radius, $r + dr$, and dividing this by the average number of fibres per unit area. It can be mathematically defined as,

$$G(r) = \frac{1}{N_a(2\pi r)} \cdot \frac{dK(r)}{dr} \quad (1)$$

where, $dK(r)$ is the average number of fibre centres lying within an annulus of inner radius, r, and outer radius, $r + dr$, and N_a is the number of fibres per unit area [7]. The radial distribution function, shown in Fig. 3a, exhibits a large peak at a distance of 7 μm, which coincides with the peak seen in the 1st nearest neighbour distribution function (shown in Fig. 2b). For the medium range (i.e. 10 μm $\leqslant r \leqslant$ 25 μm), the function exhibits some fluctuations, typical of a high volume fraction composite. At the long range (i.e. $r > 25$ μm), the function approaches unity as the value of r becomes large enough to be representative of the overall region.

2.1.3. Second-order intensity function

The second-order intensity function, also known as Ripley's K-function, is widely used to distinguish between different types of point patterns [11,12]. The function $K(r)$ is defined as the number of further points expected to lie within a radial distance, r, of an arbitrary point, as shown in Fig. 1a, divided by the number of points per unit area, N_a. The boundary of the domain has a significant effect when calculating this function and an estimator which accounts for edge-correction has been established by Ripley [13],

$$K(r) = \frac{A}{N^2} \sum_{k=1}^{N} w_k^{-1} I_k(r) \tag{2}$$

where N is the total number of points in the area, A, $I_k(r)$ is the number of points lying within radial distance r of a given fibre and w_k is the ratio of the circumference lying within the area A to the whole circumference of the circle. Generally, point fields are compared against a pattern exhibiting complete spatial randomness (CSR), for which the K-function of the domain can be analytically evaluated as [12],

$$K_r(r) = \pi r^2 \tag{3}$$

Shown in Fig. 3b are the second-order intensity functions for the CFRP composite and the CSR pattern. It can be seen that the experimental curve is initially below the CSR curve and shows evidence of a slight stair-shape, which is indicative of a certain amount of regularity in the fibre arrangement at shorter distances (i.e. $r \leqslant 15$ μm). However, at larger distances (i.e. $r > 15$ μm) the curve is above and diverging away from the CSR pattern which is a result of long range clustering. It can be thus concluded that the distribution of fibres in CFRP microstructure does not conform to a CSR pattern. This then rules out the approaches outlined earlier which generated a random distribution of fibres and highlights the need to develop an approach that can recreate the spatial pattern of the actual experimental microstructure.

3. Algorithm development

Following this finding, an algorithm was developed in Matlab and its purpose was to generate a high volume fraction fibre distribution which is statistically equivalent to the actual CFRP microstructure. The importance of the short range interaction of fibres has already been highlighted and so to accurately reproduce this the algorithm uses a bottom-up approach by populating a region using an 'adjusted' measure of 1st and 2nd nearest neighbour distribution functions, shown in Fig. 2b and c, to define the distances between neighbouring fibres. The adjusted measures of the nearest neighbour distributions account for the fact that some nearest neighbour distances can be shared by two fibres and are therefore counted twice in the original distributions, such as Fibres 1 and 2 shown in Fig. 4c. In order for the newly developed algorithm to reproduce equivalent distribution functions, the nearest neighbour distances common to two fibres may only be counted once. For example, for Fibre 2, instead of using the distance to Fibre 1 (which has already been counted in the distribution as Fibre 2 is the nearest neighbour of Fibre 1), the distance between it and Fibre 3 is now counted in the adjusted nearest neighbour distribution. This follows for all fibres under consideration.

The resulting distributions exhibit very similar properties to the nearest neighbour distributions, shown in Fig. 2b and c. The adjusted first and second nearest neighbour distribution functions could both be fit to a logistic distribution curve. The algorithm then uses these logistic distribution parameters to define the inter-fibre distances for the first and second nearest neighbours of a given fibre. Fibre diameters are chosen directly from the experimentally measured fibre diameter distribution curve, shown in Fig. 2a. The algorithm, titled the nearest neighbour algorithm (NNA), follows the procedure below, which is also illustrated in Fig. 4.

1. A random point is created having coordinates (x_1, y_1), lying in a sample square area, the size of which is defined by the user. The

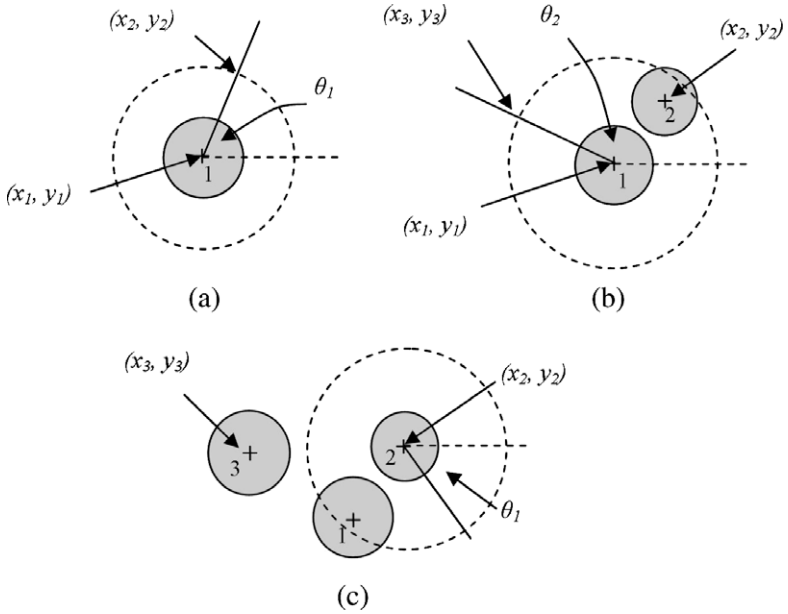

Fig. 4. (a) Assigning a fibre's nearest neighbour. (c) Assigning a fibre's second nearest neighbour. (c) Nearest neighbour being assigned for a subsequent fibre.

diameter, d_1, of the surrounding fibre is drawn from a lognormal distribution fitting the experimentally measured diameter distribution, as shown in Fig. 2a.

2. A second point is created (x_2, y_2), which is the centre of the first nearest neighbour of the previous fibre. The distance from (x_1, y_1) to (x_2, y_2) is assigned from the adjusted first nearest neighbour distribution function. The new point is oriented at a random angle θ_1, where $-\pi \geq \theta_1 \geq \pi$ (see Fig. 4a). The fibre diameter is assigned from the same lognormal distribution as before.
3. A third point is created (x_3, y_3), which is the centre of the second nearest neighbour of the first fibre. The distance from (x_1, y_1) to (x_3, y_3) is assigned from the adjusted second nearest neighbour distribution function. As before, the new point is oriented at a random angle θ_2, where $-\pi \geq \theta_2 \geq \pi$ (see Fig. 4b) and the fibre diameter is assigned from the lognormal distribution.
4. The algorithm then moves onto the second fibre and assigns its first and second nearest neighbours, for which the nearest neighbour distances are drawn from their respective distributions and fibre diameters are assigned as before (see Fig. 4c).
5. The algorithm then moves onto the third fibre and the same procedure is carried out. This process is repeated for each fibre thereafter until the sample area is filled.
6. The algorithm performs numerous checks at each iteration to ensure that none of the fibres overlap with one another and the fibres lie within the sample area chosen. If overlaps occur or a fibre is placed outside the sample area, orientation angles or inter-fibre distances are reassigned until a suitable configuration is found.
7. If no suitable configuration can be found (i.e. near a boundary or in a region saturated with fibres), the algorithm will move onto the next fibre and continue as before.
8. For any fibre crossing a boundary, a corresponding fibre is placed on the opposing boundary to maintain geometric periodicity. A fibre already situated in this area will be removed if an overlap occurs with the newly mapped fibre. However, a new fibre is subsequently reassigned a position near the mapped fibre should it be available in order to try and maintain the correct fibre volume fraction locally.

4. Statistical characterisation

In order to analyse the numerically generated microstructures, a SERVE size large enough to be representative of the bulk material must be used. The size of an SERVE can be represented by the variable δ, which relates length of the side of the SERVE L, to the fibre radius r_f, using the following simple relationship,

$$\delta = \frac{L}{r_f} \tag{4}$$

Trias et al. [14] determined that for a typical carbon fibre reinforced polymer, having a fibre volume fraction of 50%, the minimum required size of an SERVE is $\delta \geqslant 50$. The mechanical and statistical criteria considered for the analysis were the effective properties, the Hill condition, the mean and variance of stress and strain fields, probability density functions of the stress and strain components in the matrix and fibre distance distributions.

Following this study, a value of $\delta = 50$ was used to generate 25 microstructures each measuring 165 μm × 165 μm and one of these is shown in Fig. 5a. A microstructure exhibiting a periodic hexagonal array of fibres is also shown in Fig. 5b. This type of arrangement would have been the focus of many previous micromechanical investigations of composite materials [16]. The microstructure generated by the NNA is seen to reproduce short range regularity, matrix rich regions and 'lines' of fibres much the same as in the original micrograph, shown in Fig. 1a. Four regions (A, B, C and D) have been identified in both images to highlight these similarities. The statistical descriptors (discussed in Section 2) characterising these models have been derived and the mean values for these arrangements are compared to the experimentally measured statistical functions. Error bars have been included for each of the functions indicating the maximum and minimum values generated from the models for each data point and are discussed next.

4.1. Nearest neighbour distributions

Shown in Fig. 2b and c are the probability density functions for the 1st and 2nd nearest neighbour distances, respectively. As these formed some of the input parameters for the NNA, a very good correlation is found between the experimentally measured distribution and the distributions generated by the NNA, thus showing that the short range interaction of fibres is being accurately reproduced. This has important implications when modelling damage and failure in composites as the highest stresses tend to occur in regions where fibres are in closest proximity.

4.2. Radial distribution function

The radial distribution functions for both the numerically generated microstructures and the experimental microstructure are shown in Fig. 3a. Again, excellent correlation is achieved, thus confirming that the NNA is reproducing the same short and long range inter-fibre distances. The graph shows an initial high peak caused by the physical area of the inclusions, followed by a number of

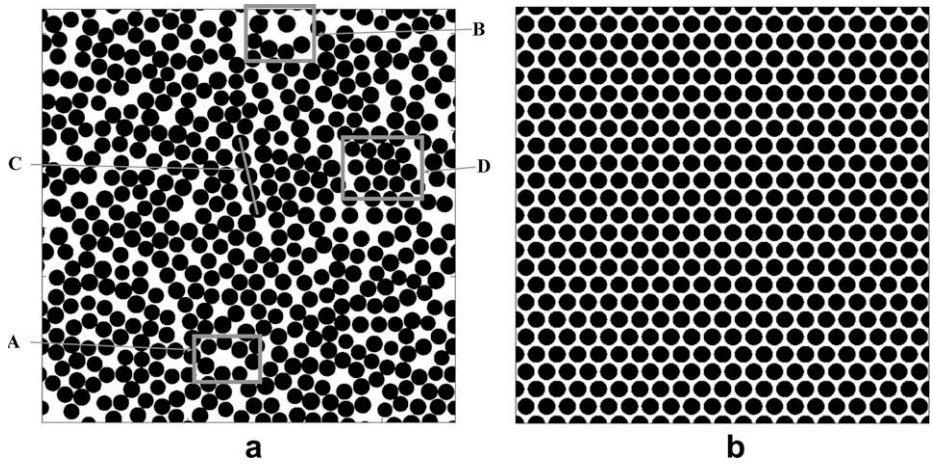

Fig. 5. (a) Generated distribution using nearest neighbour algorithm. (b) Periodic fibre distribution (hexagonal).

oscillations until, finally, the value of the plot approaches a value of unity indicating the numerically generated microstructures are statistically homogenous.

4.3. Second-order intensity function

Fig. 3b shows the second-order intensity function (Ripley's *K*-function) for the experimental microstructure and the numerically generated microstructures. Also shown is the *K*-function for a model which exhibits complete spatial randomness. Excellent agreement is seen in the type of pattern being generated by the NNA and the experimental microstructure. The NNA is able to replicate the regularity between fibres in the real microstructure at short range distances, indicated by the slight stair shape seen in the plot at smaller values of *r*. The CSR pattern does not replicate this initial stepwise increase. At larger distances the curve diverges away from the CSR pattern, reproducing the long range clustering from the experimental sample. Thus, the same spatial pattern is being produced by the NNA, for which the statistical distributions defining it are almost identical.

4.4. Volume fraction

Unlike other similar algorithms [8–9], the volume fraction of the numerically generated microstructures is not predefined. It is controlled by the experimental functions used as the input parameters, i.e. the adjusted nearest neighbour distributions and the diameter distribution of the fibres. In order to test the effectiveness of the NNA, the volume fraction has been examined over a range of RVE sizes, as shown in Fig. 3c. Twenty microstructures were generated at each value of δ and it can be seen that there is a large variance between the volume fractions produced for the smallest models (i.e. $\delta = 10$). This is due to the conditions the NNA uses when placing fibres near a boundary. For smaller models, the influence of the boundary is relatively large compared to the overall area of the RVE. The larger models, (i.e. $\delta \geqslant 20$) are seen to converge close to the experimental volume fraction of 59.2% showing very little variance in the volume fractions being produced.

5. Prediction of mechanical properties

A homogenisation procedure was used to evaluate the effective properties of the generated microstructures. Finite element models were generated in ABAQUS [15] and used to impose periodic boundary conditions as described in [16,17] to an RVE which enable the relevant modes of deformation of the composite to be simulated. A two-dimensional generalised plane strain model was used to determine the longitudinal modulus E_{11} from the models, using three-noded generalised plane strain elements (CPEG3). The in-plane properties were determined with a two-dimensional plane strain model using three-noded plane strain elements (CPE3). The effective elastic properties were evaluated based on the relevant stress–strain ratio for a given loading condition. In order to evaluate the average stresses ($\bar{\sigma}_{ij}$) and strains ($\bar{\varepsilon}_{ij}$) over the RVE, the following equations were used [16,17],

$$\bar{\sigma}_{ij} = \frac{1}{V}\sum_{k=1}^{n}\left(\sigma_{ij_k}V_k\right) \tag{5}$$

$$\bar{\varepsilon}_{ij} = \frac{1}{V}\sum_{k=1}^{n}\left(\varepsilon_{ij_k}V_k\right) \tag{6}$$

where V is the total volume of the RVE, k is the element number, V_k is the volume of element k in the finite element mesh, n is the total number of elements and σ_{ij_k} and ε_{ij_k} are the ij stresses and strains, in element k, respectively. Elastic modulus in the relevant direction was then calculated by dividing the average stress (Eq. (5)) by the average strain (Eq. (6)).

Effective properties were calculated for numerically generated microstructures of increasing size using the homogenisation procedure. Twenty microstructures were generated using the NNA at each value of δ. Fig. 6a and b shows the mean values of the homogenised elastic properties. Error bars have been included indicating the maximum and minimum values calculated at each value of δ. The results show similar trends to the volume fraction study carried out (Fig. 3c), with a large variance evident at low values of δ as a result of the wide range of volume fractions. It was determined that the in-plane elastic properties converge to a constant value when $\delta = 20$ where it was found that the maximum and minimum values of all 20 generated microstructures fell within 10% of the mean values. The mean homogenised effective properties of the largest models (i.e. $\delta = 50$) compare well with experimentally measured elastic properties [18] shown in Fig. 6a and b. At high values of δ, very little variance in elastic properties is seen for all generated models, with the maximum and minimum values falling within 3% of the mean values. As a comparison, effective properties have also been determined for periodic hexagonal fibre arrays (with same V_f) at each value of δ, and these are also shown in Fig. 6. As can be seen these hexagonal models predict the same effective properties for all values of δ, to which the properties predicted by the NNA converge. However, the peak stresses in the NNA models were found to be 92% higher than those in the periodic models, suggesting that accurate predictions of both damage initiation and overall failure of the material is highly dependant on the type of fibre distribution used in a micromechanical model. Finally, Fig. 6b also shows that the numerically generated micro-

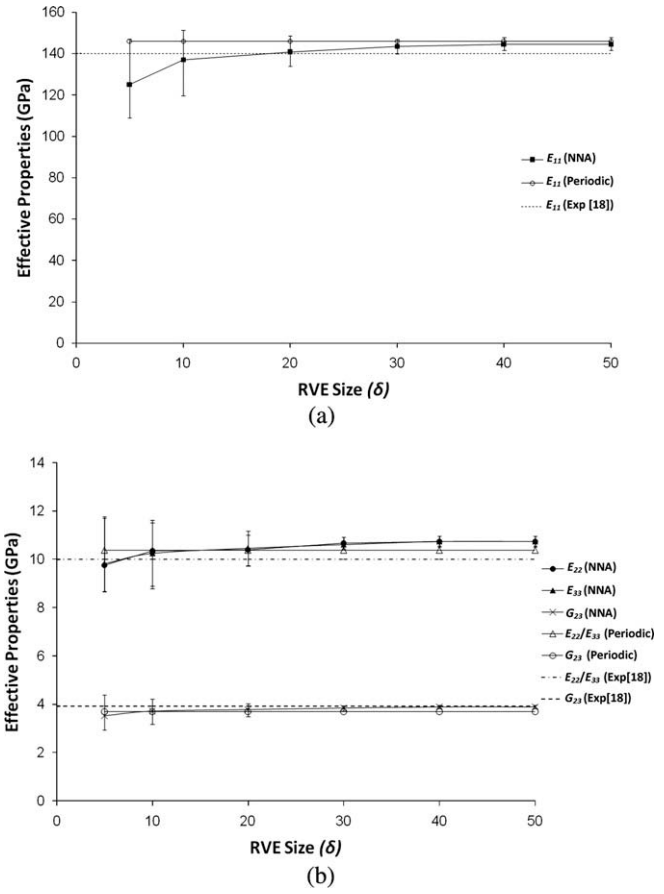

Fig. 6. (a) Elastic properties in longitudinal direction. (b) In-plane elastic properties of numerically generated microstructures.

structures are transversely isotropic due to fact that E_{22} and E_{33} converge to the same value for the largest models.

6. Concluding remarks

A novel method has been developed in order to generate accurate representations of a composite material microstructure with a high volume fraction. The microstructure of a CFRP composite was experimentally characterised in terms of fibre volume fraction, fibre diameter and also statistical distributions describing the fibre arrangement. It was found from the experimental analysis that CFRP microstructure had a fibre distribution which was not characterised by a CSR pattern. This highlighted the need for an experimental approach to be used to generate accurate fibre distributions. Using the experimentally measured data, an algorithm was developed which can generate fibre distributions with high volume fractions and the same geometric features as the experimental samples, as determined using statistical analysis. The NNA uses an adjusted measure of the experimentally measured 1st and 2nd nearest neighbour distribution functions to define inter-fibre distances. The key factor to avoid jamming of the microstructure (as seen in [6,8]) was to assign both the 1st and 2nd nearest neighbours at each step in the process. Assigning only the first nearest neighbour was found not to produce the desired fibre distribution as it was also subject to a jamming limit at ~55%. Fibre diameters are assigned using the experimentally measured diameter distribution. Upon statistical analysis, the NNA was found to produce distributions which were statistically equivalent to the real microstructure, accurately reproducing both the short and long range interaction of fibres.

Using finite element analysis, effective properties of the generated microstructures were calculated through a homogenisation procedure. The homogenised properties of the composite were found to show good agreement with the experimentally measured properties of [18]. A parametric study, in which the size of the generated microstructure was varied, was carried out and it was found that the elastic moduli converged for a microstructure window which has a side of length of approximately 20 times the fibre radius, which for this material is approximately half a ply thickness (i.e. 65 μm). Based on the results of this study it has been found that hexagonal RVE models can accurately predict the effective elastic properties of the composite. However, it has been found that peak stresses in the NNA models were 92% higher than those in the periodic models. It is thus recommended that NNA models be used in strength prediction studies and this will be reported on in a future publication.

The algorithm developed is simple, robust, highly efficient and reproduces actual fibre distributions for high strength laminated composite materials. The distribution of fibres in a composite depends heavily on the manufacturing and processing conditions, and for this reason this newly developed method provides a useful alternative to purely numerical based models that rely on the theory of random close packing and also direct microstructure reproduction. It does not require further heuristic steps, such as those seen fibre stirring/shaking algorithms, in order to achieve high volume fraction microstructures. This method can easily be applied to other types of composite materials by characterising relevant experimental distributions.

Acknowledgements

This authors wish to acknowledge the funding provided by the Irish Research Council for Science, Engineering and Technology (IRCSET) and Science Foundation Ireland (SFI).

References

[1] González C, Llorca J. Multiscale modeling of fracture in fiber-reinforced composites. Acta Mater 2006;54(16):4171–81.
[2] Swaminathan S, Ghosh S, Pagano NJ. Statistically equivalent representative volume elements for unidirectional composite microstructures: part I – without damage. J Compos Mater 2006;40(7):583–604.
[3] Trias D, Costa J, Mayugo JA, Hurtado JE. Random models versus periodic models for fibre reinforced composites. Comput Mater Sci 2006;38(2):316–24.
[4] Hojo M, Mizuno M, Hobbiebrunken T, Adachi T, Tanaka M, Ha SK. Effect of fiber array irregularities on microscopic interfacial normal stress states of transversely loaded UD-CFRP from viewpoint of failure initiation. Compos Sci Technol 2009;69(11–12):1726–34.
[5] Pyrz R. Correlation of microstructure variability and local stress-field in 2-phase materials. Mater Sci Eng A 1994;177(1-2):253–9.
[6] Buryachenko VA, Pagano NJ, Kim RY, Spowart JE. Quantitative description and numerical simulation of random microstructures of composites and their effective elastic moduli. IJSS 2003;40(1):47–72.
[7] Yang S, Tewari A, Gokhale AM. Modeling of non-uniform spatial arrangement of fibers in a ceramic matrix composite. Acta Mater 1997;45(7):3059–69.
[8] Melro AR, Camanho PP, Pinho ST. Generation of random distribution of fibres in long-fibre reinforced composites. Compos Sci Technol 2008;68(9):2092–102.
[9] Wongsto A, Li S. Micromechanical FE analysis of UD fibre-reinforced composites with fibres distributed at random over the transverse cross-section. Compos Part A – Appl Sci 2005;36(9):1246–66.
[10] Trias D. Analysis and simulation of transverse rando fracture of long fibre reinforced composites. Ph.D. Thesis, University of Girona, Dep. dEnginyeria Mecanica i de la Construccio Industrial; 2005.
[11] Pyrz R. Quantitative description of the microstructure of composites part 1: morphology of unidirectional composite systems. Compos Sci Technol 1994;50(2):197–208.
[12] Diggle P. Statistical analysis of spatial point patterns. London: Arnold; 2003.
[13] Ripley BD. Modelling spatial patterns. J Roy Stat Soc Ser B (Stat Method) 1977;39(2):172–212.
[14] Trias D, Costa J, Turon A, Hurtado JE. Determination of the critical size of a statistical representative volume element (SRVE) for carbon reinforced polymers. Acta Mater 2006;54(13):3471–84.
[15] ABAQUS, Version 6.7. HKS; 2007.
[16] Keane A, McCarthy CT, O'Dowd NP. The effect of matrix non-linearity on the properties of unidirectional composite materials for multi-scale analysis. In: Proceedings of the ninth international conference on computational structures technology. Athens, Greece: Civil-Comp Press; 2008. p. 312.
[17] Van der Sluis O, Schreurs PJG, Brekelmans WAM, Meijer HEH. Overall behaviour of heterogeneous elastoviscoplastic materials: effect of microstructural modelling. Mech Mater 2000;32(8):449–62.
[18] O'Higgins RM, McCarthy MA, McCarthy CT. Comparison of open hole tension characteristics of high strength glass and carbon fibre-reinforced composite materials. Compos Sci Technol 2008;68(13):2770–8.